

Received June 30, 2019, accepted July 13, 2019, date of publication August 2, 2019, date of current version August 19, 2019.

Digital Object Identifier 10.1109/ACCESS.2019.2932800

# Comprehensive Study on RF-MEMS Switches Used for 5G Scenario

LI-YA MA<sup>1,2</sup>, NORHAYATI SOIN<sup>1,2</sup>, (Member, IEEE), MOHAMAD HAZWAN MOHD DAUT<sup>2</sup>, AND SHARIFAH FATMADIANA WAN MUHAMAD HATTA<sup>1,2</sup>, (Member, IEEE)

<sup>1</sup>Department of Electrical Engineering, Faculty of Engineering, University of Malaya, Kuala Lumpur 50603, Malaysia

<sup>2</sup>Centre of Printable Electronics, University of Malaya, Kuala Lumpur 50603, Malaysia

Corresponding author: Li-Ya Ma (maliya8445@gmail.com)

This work was supported in part by the University of Malaya through the Faculty Fund under Grant RF024A-2018(UM.0000482/HRU.OP.RF).

**ABSTRACT** This paper presents a comprehensive study on radio frequency-microelectromechanical systems (RF-MEMS) switches, which are expected to be extensively integrated into 5G infrastructures. The specifications of the RF-MEMS switch in use case and scenario for 5G have been summarized in part 2 and followed by the study of the state-of-the-art RF-MEMS switches in part 3. Both metal-contact and capacitive RF-MEMS switches, which have been developed and fabricated within the last two decades, are studied and tabled. In order to meet with the specification requirements of 5G scenario, the performance and characteristics of the RF-MEMS switches should be enhanced, such as acceptable RF performance, low actuation voltage, good reliability, short switching time, multiband topology, and on-chip integration and packaging. Different techniques for the improvement of the RF-MEMS switches' properties, for instance low spring constant, large actuation area, diverse actuation methods, push-pull mechanism, modified driving voltage waveform, inductive compensation, and so on, have been thoroughly investigated, classified, and summarized in part 4, which serves as the main contribution of the review. The findings from this review can be beneficial for further RF-MEMS switches' design and improvement. The upgraded RF-MEMS switches are capable of satisfying the growing need of cutting edge performance for 5G or high-performance applications.

**INDEX TERMS** 5G, RF-MEMS switch, high performance, different techniques.

## I. INTRODUCTION

In mobile wireless communication systems, 5G stands for the fifth Generation mobile technology. Comparing to the previous communication technologies (e.g., 1G, 2G, 3G, and 4G), 5G will be significantly improved in terms of incredibly high data volume and rate, tremendous number of connected devices, shorter end-to-end (E2E) latency and very wide frequency bandwidth. With the emerging and development of IoT (Internet of Things) which will ultimately connect any objects and environment entities in our daily life experience, earning their own identities in the digital world, by means of the Internet, 5G systems are expected to be the enabler since it is capable to deliver up to 1000 times the capacity of current mobile networks. With this new technology implemented and employed by an extensive

class of components, such as wideband switches, switching units, multi-state impedance tuners, and multi-state phase shifters, reconfigurable filters, programmable step attenuators, hybrid devices, as well as miniaturized antennas and arrays, these components will require an upgrade on their own to support the superior performance of 5G networks [1]. The key RF (radio frequency) subsystems in 5G RF transceiver include antennas, tunable filters, RF power amplifiers, and MIMO (multiple-input multiple-output) [2]. In all of these 5G systems or subsystems, it can be seen that, from the hardware aspect, RF switch is one of the most fundamental and crucial component which is used to route signals through transmission paths with a high degree of efficiency; its RF characteristics, switching time, power handling and reliability can directly affect the related properties and performance of the 5G applications.

There are many commercial RF switches developed and available in the market so far. For example, pHEMT

The associate editor coordinating the review of this manuscript and approving it for publication was Hamid Mohammad-Sedighi.

(pseudomorphic high electron mobility transistor) from Skywork<sup>®</sup> [3] exhibits low insertion loss, high isolation and linearity, as well as good power handling; but its operation frequency range is limited up to 8GHz. Electromechanical relay RF switches from Pasternack Enterprises<sup>®</sup> presents very low insertion loss, high isolation and power handling in the wide millimeter wave frequency range; however, it has very limited lifetime, large assembly and high actuation voltage [4]. Solid-state RF switches, such as high-speed silicon p-i-n diode or FET (field-effect transistor), also from Pasternack Enterprises<sup>®</sup> present long lifetime, fast switching speed, and good isolation in wide mm-wave frequency range; but have relatively limited insertion loss especially in the kilohertz range [4]. Keysight Technologies, Inc.<sup>®</sup> proposes several electromechanical switches, e.g., multipoint switches, SPDT (single-pole double-throw) switches, bypass switches, matrix switches, and so on, with pretty good RF characters [5]; however, their very high operation voltages are not practical with mobile or green cellular system.

The field of micro electromechanical systems (MEMS) for radio frequency (RF) applications, known as RF-MEMS, has been gathering interest since early discussions in scientific literatures about two decades ago [6]. RF-MEMS switches with acceptable performance are now becoming available in the market [7], such as the RF-MEMS switches from Omron and Radant [8] where hybrids and band pass filters are employed to form a novel Frequency dependent power limiter circuit [9], [10]. RF-MEMS switches are also integrated into transmitters and receiver circuits within cellular base stations in telecommunication networks where it is used in switching filters to access different bands of frequencies without rebooting the system [11]. It is predicted that RF-MEMS switches can be good alternatives and play an important role in mobile communications due to the increase in demand of high-speed internet connectivity which has led to rapid deployment of 5G network infrastructures [12], [13]. This is because comparing to the conventional RF switches, RF-MEMS switches exhibit many significant advantages, such as negligible power consumption, less series capacitance and resistance, very high cut-off frequency, good isolation and high linearity in a very wide frequency range [14], [15]. Also, with recent substantial efforts in developing low-voltage RF-MEMS switch, the technology can be easily implemented into remote, wireless, or green automatic systems. Besides these remarkable characteristics, replacing the standard counterparts by RF-MEMS switches in RF systems can reduce the hardware complexity which can in turn reduce its cost and lead times, as well as system's power consumption; the transceiver operability, on the other hand, can be extended according to multiple standards and services [16].

Iannacci *et al.* has figured out how 5G high-level characteristics reflect in terms of demands and expected performances of RF devices [16], [17]. In this review, we have summarized the design specifications of the RF-MEMS switch used for 5G scenario in part 2 and followed by the literature review

on the state-of-the-art RF-MEMS switch designs within the last twenty years in part 3. Subsequently, the different technologies from these designs for the improvement of the RF-MEMS switch's specific properties are investigated and summarized in order to suit better with the 5G scenario's specifications, as illustrated in part 4. This is then followed by the conclusion on how from existing architectures and specifications of the RF-MEMS switch can be enhanced even more in terms of design and performance. Many review papers on RF-MEMS switches have been reported before; however, to the best of our knowledge, this is the first paper to review RF-MEMS switches for 5G scenario in terms of improving their corresponding properties by different technologies which can be a main reference for new RF-MEMS switch's development or improvement especially used for 5G infrastructures or higher-level applications.

## II. SPECIFICATIONS OF RF-MEMS SWITCHES FOR 5G SCENARIO

It is envisaged that 5G will seamlessly integrate the existing Radio Access Technologies (e.g., GSM – global system for mobile communications, HSPA – high speed packet access, LTE – long term evolution and WiFi – wireless fidelity) with complementary new technologies invented for millimeter wave bands [2]. This envisagement shows that comparing to the existing technologies, 5G system demands for wider and higher operation frequency range, as well as larger reconfigurability to cover different services, and can meanwhile reduce hardware redundancy and power consumption [18]. Millimeter wave technology used for 5G systems not only can provide plenty of available spectrums at this band, but also can diminish antenna sizes, fulfill the fabrication of array antennas with hundreds or thousands of antenna elements at wireless nodes or equipment. Smart antennas with beam forming and phased array capabilities will be employed to point out the antenna beam to a desired location with high precision, and rotated electronically through phase shifting [2] – thence realized by employing high-quality RF-MEMS switches and transmission lines.

It is necessary to define how 5G systems' characteristics will reflect in terms of demands and expected performances of RF-MEMS switches. According to the 5G system architecture [2], the characteristics and performances of its subsystems, the specification requirements of the RF-MEMS switches used for these 5G scenarios are as below [1], [12], [16], [17], [19].

*Frequency range:* low-frequency band which is below 6GHz (e.g., 3.3~4.2GHz, 4.4~5GHz); and high-frequency band which is in the range of 24.25~27.5GHz and 37~43.5GHz for China, 27.5~28.28GHz for Japan, 26.5~29.5GHz for Korea, 27.5~28.35GHz, 37~40GHz and 64~71GHz for US, and 24.25~27.5GHz for Europe;

*Isolation:* better than  $-30 / -40$ dB for frequencies as higher as possible;

*Insertion loss:* less than 1dB on the widest possible frequency range;

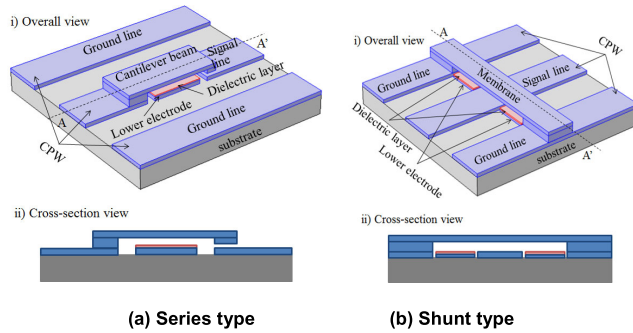


**FIGURE 1.** Typical structures of metal-contact RF-MEMS switch [22].

*Switching time:* lower than 1ms, with few fractions of  $\mu\text{s}$  (e.g., 200~300 $\mu\text{s}$ ) as reasonable target;

*Control voltage:* within a few volts (e.g., 2 ~ 3V);

*Lifetime (or reliability):* more than 1 billion ( $10^9$ ) switching cycles;

*Packaging and integration:* compatible with standard CMOS (Complementary Metal-Oxide-Semiconductor Transistor) technologies.

### III. LITERATURE REVIEW ON STATE-OF-THE-ART RF-MEMS SWITCHES

RF-MEMS switches, in general can be realized by two different contact mechanisms, either metal-contact type (namely metal-to-metal contact) or capacitive type (namely metal-insulator-metal contact). Metal-contact RF-MEMS switches present good performance in the frequency range of tens MHz to tens GHz [20]; their isolation is basically limited by the parasitic capacitance; and insertion loss is determined by the contact resistance. In contrast, capacitive RF-MEMS switches can operate in a wider frequency range, typically from few GHz to hundreds GHz and exhibit better performance at a higher frequency range [21]. By referring to the specification of the frequency range which is mentioned in the previous section, both metal-contact and capacitive RF-MEMS switches can be considered as good candidates to be implemented into the 5G scenario.

#### A. METAL-CONTACT RF-MEMS SWITCHES

Fig.1 [22] shows typical structures of metal-contact RF-MEMS switch which are actuated by electrostatic force. With applied voltage between the cantilever beam (or membrane) and the lower electrode, the switch can be actuated via the induced electrostatic force between two electrodes; and the suspended part will have direct contact to the signal line. For the series metal-contact RF-MEMS switch, as shown in Fig. 1(a), the RF signal can be passed through the CPW (coplanar waveguide) transmission line, namely switch-on state, when the switch is actuated. As for the shunt-type switch, as shown in Fig. 1(b), the RF signal would be bypassed to the ground line, namely switch-off state, when the switch is actuated; and vice versa. These switches use

metal-to-metal contact (or ohmic contact) between the signal line and suspended electrode.

There have been many metal-contact RF-MEMS switches developed and reported so far, with different design structures, fabrication methods and properties. For example, a single-crystalline silicon (SCS) metal-contact RF-MEMS switch was designed and fabricated using a silicon-on-glass (SiOG) substrate [23], [24], in order to lower the fabrication cost and obtain high productivity and uniformity, as well as good RF, mechanical and electrical properties; the lifetime of the switch can reach more than  $10^8$  switching cycles with power handling higher than 1W; the actuation voltage of 10.7V was obtained which exceeds the 5G specification. Chu *et al.*, proposed an electrostatically RF-MEMS switch by means of exploiting buckling and bending effects with novel crisscross-shape suspended electrode [25], where the residual stress of the dielectric layer (namely aluminum nitride film) was controlled to obtain a desirable structure with center-buckled fixed-fixed beam and free-end bended cantilever beams. The switch shows good insertion loss ( $-0.21\text{dB}$ ) and isolation ( $-44\text{dB}$ ) at frequency of 5GHz, but at the expense of a bit high actuation voltage of 10.2V. A wide band compact RF-MEMS switch based on series-shunt topology with three identical metal-contact switch cells was fabricated and measured in [26]; it shows that the switch can be operated from DC to 12GHz, with isolation of higher than 40dB, insertion loss of less than 0.3dB, switching time of 47 $\mu\text{s}$  within the design area of 1mm $\times$ 1.2mm, however large actuation voltage of 20 to 40V. Patel *et al.*, presented an electrostatic RF-MEMS switch with high reliability ( $>100$  million cycles), high-power handling ( $>10\text{W}$ ) and high-linearity (IIP3 $>69\text{dBm}$ ) for DC to 40GHz applications by using a thick suspended plate (around 10 $\mu\text{m}$ ) and four curved springs, which also exhibits less sensitivity to biaxial stress, temperature and stress gradients. However, the switch requires high actuation voltage (at least larger than 68V) [27], [28]. Wang *et al.*, proposed a novel laterally-movement electrostatic RF-MEMS switch with three states, (namely switch-on, switch-off and deep-switch-off) by using a rhombic membrane and two groups of differential parallel plate actuators [29], which presents a low insertion loss ( $<0.5\text{dB}$ ) and a high isolation ( $>50\text{dB}$ ) in the frequency range of DC to 10GHz, except quite high actuation voltage of 78V. A novel niobium-based superconducting series-type RF-MEMS switch was introduced and analyzed by Attar *et al.* [30] which was fabricated using a standard superconducting microelectronics (SME) technology followed by several post-processing steps, shows the possibility of RF-MEMS switch operating at cryogenic temperature (e.g., 4K) and exhibits with low insertion loss ( $<0.2\text{dB}$ ) and high isolation ( $>30\text{dB}$ ) up to 10GHz, but the actuation is around 46V. Sun *et al.* proposed a RF-MEMS switch based on thermal buckle-beam structure in [31] which can be operated in a wide temperature range of  $-20^\circ\text{C}$  to  $100^\circ\text{C}$  and demonstrates reasonable properties of insertion loss ( $<0.45\text{dB}$ ) and isolation ( $>20\text{dB}$ ) from DC to 20GHz but also needs large

**TABLE 1.** State-of-the-art metal-contact RF-MEMS switch designs.

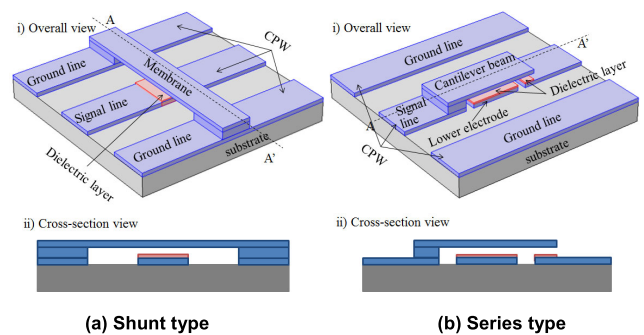
| RF-MEMS switch                   | Chan <i>et al.</i> , 2003 [33]        | Kim <i>et al.</i> , 2004 [23]                                       | Lee <i>et al.</i> , 2005 [34]                    | Seki <i>et al.</i> , 2006 [35]                       | Chu <i>et al.</i> , 2007 [25]             | Ke <i>et al.</i> , 2008 [20]                                      | Yu <i>et al.</i> , 2009 [26]   | Kim <i>et al.</i> , 2010 [24]                                       |
|----------------------------------|---------------------------------------|---|--|--|---|---|--------------------------------|---|
| Structure                        |                                       |   |  |  |   |   |                                |   |
| Frequency range                  | 0.25–40GHz                            | DC–30GHz  | 0.5–20GHz  | 2–4GHz   | DC–10GHz                                  | DC–15GHz  | DC–12GHz                       | DC–15GHz  |
| Isolation                        | >20dB                                 | -38.8dB@2GHz  | -30.6dB@20GHz                                    | -48dB@4GHz   | -44dB@5GHz                                | -30dB@4GHz  | -56.2dB@6GHz                   | -41.25dB@2GHz   |
| Insertion loss                   | <0.1dB                                | -0.18dB@2GHz  | -0.19dB@20GHz                                    | -0.94dB@4GHz   | -0.21dB@5GHz                              | -0.7dB@4GHz   | -0.18dB@6GHz                   | -0.13dB@2GHz  |
| Switching time                   | <22μs                                 | 25μs  | 8μs  | 300μs  | ---                                       | 176μs   | 47μs                           | ---   |
| Control voltage                  | 14.4V                                 | 26V   | 27.5V  | 24V  | 10.2V                                     | 36V   | 28V                            | 10.7V   |
| Lifetime                         | 7×10 <sup>9</sup> cycles <sup>A</sup> | 10 <sup>8</sup> cycles <sup>B</sup>                                 | ---  | >10 <sup>9</sup> cycles <sup>B</sup>                 | ---                                       | 10 <sup>8</sup> cycles <sup>B</sup>                               | ---                            | ---   |
| Monolithic integrated compatible | Yes                                   | Yes   | Yes  | No   | Yes                                       | No  | Yes                            | Yes   |
| Fabrication technology           | Compatible with GaAs MMIC process     | Single-crystalline silicon (SCS) Fabricated using an SiOG substrate | Surface micromachining process on GaAs substrate | Glass process and SOI process with an anodic bonding | Surface micromachining on glass substrate | Surface and bulk micromachining processes with full-wafer bonding | Surface micromachining process | Single-crystalline silicon (SCS) Fabricated using an SiOG substrate |

| RF-MEMS switch                   | Yamane <i>et al.</i> , 2011 [36]  | Patel <i>et al.</i> , 2012 [28]          | Wang <i>et al.</i> , 2013 [29]                                 | Attar <i>et al.</i> , 2014 [30]                      | Sun <i>et al.</i> , 2015 [31]  | Wipf <i>et al.</i> , 2016 [32] | Liu <i>et al.</i> , 2017 [37]                              | Iannaci, 2018 [6]   |
|----------------------------------|---|--|--|--|--------------------------------|--------------------------------|--|---|
| Structure                        |   |  |  |  |                                |                                |  |   |
| Frequency range                  | 12GHz   | 0.1–40GHz                                | 0.1–10GHz  | 10MHz–10GHz  | 0–20GHz                        | 110–170GHz                     | Up to 40GHz  | Up to 110GHz  |
| Isolation                        | 51.4dB  | -22dB@20GHz                              | -53dB@6GHz   | >20dB  | >20dB                          | -36dB@140GHz                   | 36dB   | >15dB   |
| Insertion loss                   | 0.56dB  | -0.8dB@20GHz                             | -0.38dB@6GHz   | <0.2dB   | <0.45dB                        | -0.46dB@140GHz                 | 0.43dB   | <1dB  |
| Switching time                   | 30–40μs   | <10μs                                    | 72μs   | ---  | ---                            | <10μs                          | 30–40μs  | ---   |
| Control voltage                  | 85V   | 68V                                      | 78V  | 46V  | 90V                            | 50V                            | 60V  | 50V   |
| Lifetime                         | -   | >10 <sup>9</sup> cycles <sup>A</sup>     | ---  | ---  | ---                            | ---                            | 5×10 <sup>7</sup> cycles <sup>B</sup>                      | 10 <sup>8</sup> cycles <sup>B</sup>                               |
| Monolithic integrated compatible | Yes   | Yes                                      | No   | Yes  | Yes                            | Yes                            | No   | Yes   |
| Fabrication technology           | DRIE for SOI wafer both sides & Au electroplating for waveguide with four photo masks | All-metal surface micromachining process | SOG process by using an anodic bonding between silicon & glass | Standard superconducting microelectronics technology | Surface micromachining process | IHPs 0.13μm BiCMOS technology  | All-metal process with gold, platinum, titanium & chromium | Surface micromachining process with electroplated Au for membrane |

<sup>A</sup>: cold-switching condition  
<sup>B</sup>: hot-switching condition

actuation voltage of 90V. Wipf *et al.*, fabricated a SPDT switch based on a tee junction connected with two RF-MEMS switches using IHPs 0.13μm BiCMOS technology [32]. It is the first metal-contact RF-MEMS switch working in D-band (110~170GHz) which enables the integration with other analog and digital electronics on a signal chip and exhibits with reasonable isolation of higher than 18.25dB and short switching time of less than 10μs however its insertion loss is higher than 1.23dB and actuation voltage is around 50V.

Table 1 summarizes the typical design and development of RF-MEMS metal-contact switches since 2003. From these switches, it can be seen that: i) in the aspect of the connection to the transmission line, there are the shunt-type switch [23], [24], [33], series-type switch [6], [25], [30], and hybrid-type (namely series-shunt-type) switch [26]; the series-type switch also can be classified into the in-line series-type switch [6] and out-line series-type switch [25], [30]; ii) in terms of mechanical structure, the suspended electrode of the switch can be designed with cantilever beams [6], [25], [30], clamped-clamped beam, diverse-shapes of membranes with different beams [23], [24], [33], or diaphragm [20]; iii) regarding to the movement direction, the moveable electrode can be operated in either vertical direction [6], [20], [23], [25], [26], [33]–[35] or horizontal direction [29], [36], of which the former being a more popular approach; iv) from the working frequency range

**FIGURE 2.** Typical structures of capacitive RF-MEMS switch [22].

aspect, most metal-contact RF-MEMS switches are operated within 15GHz [20], [24]–[26], [29], [30], [35], [36], several switches can reach up to 40GHz [28], [33], [37]; one particular design was developed to work within 110 to 170GHz [32]; v) for an effective monolithic integration, a large proportion of the RF-MEMS switches employs the electrostatic-actuated mechanism which is of high compatibility to standard IC processes, negligible power consumption, high switching speed and simple implementation [24], [25], [38].

## B. CAPACITIVE RF-MEMS SWITCHES

Fig. 2 [22] illustrates the typical structures (shunt-type and series-type) of capacitive RF-MEMS switches which are

actuated by electrostatic force. These structures are suitable for high-frequency ( $>10\text{GHz}$ ) applications. The RF-MEMS capacitive switch is more likely to employ the shunt-type structure since it has less parasitic effect when the switch is actuated. In shunt capacitive RF-MEMS switch, the switch's impedance is varied by the coupling capacitance's changing. In switch-on state, the bridge is suspended in its original position and there is an air gap existing between the two electrode plates; thus the up-state capacitance is small which results in a high impedance between input and ground. In switch-off state, the membrane is pulled down to the signal line and there is only a very thin dielectric layer between the two electrode plates; thus resulting in a large down-state capacitance which in turn leads to a small impedance between input and ground. The basic principle of a capacitive RF-MEMS switch is thence a function of "state-off/state-on" capacitance ratio [39], which is considered to be a crucial figure-of-merit (FOM) and should be as high as possible [12], [40]–[42].

Various RF-MEMS capacitive switches with diverse structures and characteristics have been proposed and developed in the last two decades. For example, an electrostatic RF-MEMS switch with high power-handling capability of  $0.8\text{W}$  was presented in [38], where the low actuation voltage of  $6\text{V}$  and insertion loss of  $-0.17\text{dB}$  at  $40\text{GHz}$  was achieved by using serpentine beams and push-pull configuration, but the isolation is not very large ( $-15.5\text{dB}@40\text{GHz}$ ). Another type of push-pull RF-MEMS switch to realize low actuation voltage of  $8$  to  $10\text{V}$  while maintaining high power capability by using symmetric toggle mechanism was developed by Rangra *et al.* [43]. The push-pull mechanism is self-biasing and external vibrations makes it more robust, compared to the conventional RF-MEMS switch design; RF performance, however, has to be compromised. Another high power-handling (namely up to  $12\text{W}$  under how switching condition) RF-MEMS capacitive switch was proposed in [44] which showed low sensitivity to both in-plane stress, stress gradients, and temperature changes in the range of  $25^\circ\text{C}\sim 125^\circ\text{C}$ . However, it presented a low isolation of less than  $12\text{dB}$  due to the relatively large actuation area and small capacitance ratio of  $5$ . Dai *et al.*, had fabricated several capacitive RF-MEMS switches with low-actuation voltage using the commercial  $0.35\mu\text{m}$  DPFM (double polysilicon four metal) CMOS process and maskless wet-etching post process [45]–[47], where serpentine beams were used to reduce the actuation voltage to  $7\text{V}$  [46]; series inductors were added to improve the RF performance, namely insertion loss of  $-1.7\text{dB}$  and isolation of  $-19\text{dB}$  at  $21\text{GHz}$  [47]. However, due to the low resistivity of silicon substrate used in the standard CMOS process, the RF performance is not satisfactory. An under trench in the silicon substrate was thence suggested. A unique design for RF-MEMS capacitive switch with actuation voltage as low as  $4.5\text{V}$ , lifetime of  $200$  billion cyclic actuation under cold-switching condition and short switching time (namely  $<1\mu\text{s}$ ) was fabricated in 2006 [48]. As compared to the conventional design, the moveable

electrode of the switch is totally free from any anchor, pulled up by electrostatic force to turn on the switch and released back by the gravitational force to turn off the switch without any elastic deformation. The only limitation of the switch is that it must be operated at a predefined angle range ( $<28^\circ$ ) to maintain its good performance. Park *et al.*, fabricated a unique non-contact capacitive shunt RF-MEMS switch by using comb-based variable capacitors between the ground line and the signal line in [49]. A RF-MEMS shunt capacitive switch operated in V-band, namely  $40\sim 75\text{GHz}$ , was fabricated with satisfactory RF performance (isolation  $>40\text{dB}$  and insertion loss  $<0.65\text{dB}@61\text{GHz}$ ) for 5G scenario; however, the fabrication process, materials, and pull-in voltage is not compatible with standard CMOS processes [50]. Demirel *et al.* [51] developed a RF-MEMS capacitive switch which was fabricated on quartz wafer by using surface micromachining process with a new amorphous silicon (a-Si) sacrificial layer; its insertion loss and isolation is  $-0.2\text{dB}$  and  $-35\text{dB}$  respectively, at frequency of  $35\text{GHz}$ ; actuation voltage was  $28$  to  $29\text{V}$ . Li *et al.* [52] developed an electrostatic-actuated RF-MEMS capacitive switch by using actuation electrodes separated from the signal line to decouple the DC voltage and RF signals and also to reduce the up-state capacitance effect to the insertion loss. The insertion loss and isolation of the developed switch is  $-0.29\text{dB}$  and  $-20.5\text{dB}$  at  $35\text{GHz}$ , respectively; but its actuation voltage is also a bit high ( $18.3\text{V}$ ). Kumar *et al.* had fabricated a RF-MEMS shunt capacitive switch with relatively high reliability ( $\sim 10^9$  cycles of operations) and low actuation voltage ( $10\text{V}$ ) by using novel concept of tri-layer membrane; however its insertion loss and isolation is only  $1.94\text{dB}$  and  $18\text{dB}$  at the frequency range of  $100\text{MHz}$  to  $40\text{GHz}$  [53]. Shekhar *et al.* presented an RF-MEMS switch with low-control voltage ( $4.8\text{V}$ ) for millimeter-wave 5G applications in [12]. The switch can be operated in a wide frequency range of  $10\text{MHz}$  to  $60\text{GHz}$ , with low insertion loss ( $<0.6\text{dB}$ ) and high isolation ( $>20\text{dB}$ ). However, the reliability of the switch is only  $10$  million switching cycles.

Table 2 lists the state-of-the-art RF-MEMS capacitive switch designs within the last twenty years. From this table, it can be seen that: i) most capacitive RF-MEMS switches are operated in a wider and higher frequency range, compared to metal-contact RF-MEMS switches; ii) electrostatic actuation is still the most popular mechanism employed by the capacitive RF-MEMS switches; iii) a large amount of capacitive switches is proposed with large actuation membranes and different anchors; and iv) the moveable electrode of RF-MEMS capacitive switch also can be designed into vertical or horizontal movement.

#### IV. DIFFERENT TECHNIQUES FOR RF-MEMS SWITCH PERFORMANCE'S IMPROVEMENT

The previous section has listed many typical RF-MEMS switches developed in the last twenty years. Comparing their electrical and mechanical properties, reliability as well as the fabrication and packaging methods with design

**TABLE 2. State-of-the-art capacitive RF-MEMS switch designs.**

| RF-MEMS switch                   | Ramadoss <i>et al.</i> , 2003 [33]             | Peroulis <i>et al.</i> , 2004 [38] | Rangra <i>et al.</i> , 2005 [43] | Dai <i>et al.</i> , 2006 [46]     | Dai <i>et al.</i> , 2007 [47]     | Fernández <i>et al.</i> , 2008 [20] | Park <i>et al.</i> , 2009 [49]                                 | Fouladi & Mansour, 2010, [61]     |
|----------------------------------|--|------------------------------------|----------------------------------|-----------------------------------|-----------------------------------|-------------------------------------|--|-----------------------------------|
| Structure                        |  |                                    |                                  |                                   |                                   |                                     |  |                                   |
| Frequency range                  | 12~30GHz                                       | 20~40GHz                           | 8~14GHz                          | dc~40GHz                          | 0~30GHz                           | 20GHz                               | 23.5~29GHz   | 20GHz                             |
| Isolation                        | -36dB@30GHz                                    | -15.5dB@40GHz                      | -35dB@10GHz                      | -15dB@40GHz                       | -19dB@21GHz                       | >-20dB                              | -30.1dB@24GHz  | -17.9dB                           |
| Insertion loss                   | -0.3~-0.4dB                                    | -0.17dB@40GHz                      | -0.25dB@10GHz                    | -3.1dB@40GHz                      | -1.7dB@21GHz                      | <-0.5dB                             | -0.29dB@24GHz  | -0.98dB                           |
| Switching time                   | ---  | ---                                | ---                              | 8.2μs                             | ---                               | ---                                 | 8ms  | 96μs                              |
| Control voltage                  | 90~100V  | 6V                                 | 8~10V                            | 7V                                | 13V                               | 8V                                  | 25V  | 82V                               |
| Lifetime                         | 75×10 <sup>9</sup> cycles <sup>A</sup>         | ---                                | ---                              | ---                               | ---                               | ---                                 | 10 <sup>9</sup> cycles <sup>B</sup>                            | ---                               |
| Monolithic integrated compatible | No   | Yes                                | No                               | Yes                               | Yes                               | No                                  | No   | Yes,                              |
| Fabrication technology           | Flexible printed circuit processing techniques | Surface micromachining process     | 7-mask process                   | 0.35μmCMOS+Mask-less post-process | 0.35μmCMOS+Mask-less post-process | Six-mask process                    | Silicon-on-insulator & sacrificial bulk micromachining process | TSMC0.35μm+Mask-less post-process |

| RF-MEMS switch                   | Persano <i>et al.</i> , 2011 [65]          | Badia <i>et al.</i> , 2012 [57]       | Zareie & Rebeiz, 2013 [106] | Shama <i>et al.</i> , 2014 [87] | Yang <i>et al.</i> , 2015 [44]                 | Demirel <i>et al.</i> , 2016 [51] | Muhua <i>et al.</i> , 2017 [52]           | Shekhar <i>et al.</i> , 2018 [12]     |
|----------------------------------|--|---------------------------------------|-----------------------------|---------------------------------|--|-----------------------------------|---|---------------------------------------|
| Structure                        |  |                                       |                             |                                 |  |                                   |   |                                       |
| Frequency range                  | 1~40GHz                                    | 40GHz                                 | 16GHz                       | 1~60GHz                         | 0~20GHz  | 35GHz                             | 35GHz                                     | 10MHz~60GHz                           |
| Isolation                        | -38dB@23GHz                                | -35.8dB                               | -5.2dB                      | <-20dB                          | -6dB@10GHz                                     | -35dB                             | -20.5dB                                   | >20dB                                 |
| Insertion loss                   | -0.2dB@20GHz                               | -0.68dB                               | -0.2dB                      | -0.01~-0.02dB                   | -0.2dB@10GHz                                   | -0.2dB                            | -0.29dB                                   | <0.6dB                                |
| Switching time                   | ---  | 10μs                                  | 20μs                        | 0.24~0.43μs                     | 55μs   | ---                               | 15μs                                      | 33μs                                  |
| Control voltage                  | 15~20V                                     | 12V                                   | 50~55V                      | <2V                             | 5255V  | 28~29V                            | 18.3V                                     | 4.8V                                  |
| Lifetime                         | >10 <sup>9</sup> cycles <sup>A</sup>       | 2×10 <sup>9</sup> cycles <sup>A</sup> | ---                         | ---                             | ---  | ---                               | >10 <sup>9</sup> cycles                   | >10 <sup>9</sup> cycles               |
| Monolithic integrated compatible | Yes  | Yes                                   | No                          | Yes                             | No   | No                                | No  | Yes                                   |
| Fabrication technology           | Surface micromachining on III-V technology | 7-mask microsystem technology         | UCSD fabrication process    | surface micromachining process  | Quartz substrate with UCSD fabrication process | Surface-μmachined process         | Surface-μmachined process with five masks | 4-mask surface micromachining process |

<sup>A</sup>: cold-switching condition<sup>B</sup>: hot-switching condition

specifications of the RF-MEMS switches required for 5G scenarios, as mentioned in Section 2, it can be seen that there is still a big space or gap for existing RF-MEMS switches to improve. In this section, different techniques for the improvement of the RF-MEMS switch have been investigated, classified and summarized.

### A. GOOD RF PERFORMANCE

Scattering parameters (or S-parameters) of the RF-MEMS switches generally can be used to estimate their RF performance. The most important parameters include insertion loss and isolation; and these can be theoretically calculated by (1) [54]. When the RF-MEMS switch is turned on,  $S_{21}$  indicates the insertion loss; and when the RF-MEMS switch is turned off,  $S_{21}$  represents the isolation. From (1), it can be seen that the critical factor to determine the RF-MEMS switch's insertion loss and isolation is the up-state (switch-on state) or down-state (switch-off state) capacitance values. Diverse methods have been explored to improve the insertion loss and isolation of the RF-MEMS switch, such as using series-shunt configuration [26], [29], [55]–[57], compensating the switches with extra inductor [47], [57], increasing the capacitance ratio [58], and so on. Followings are the summary of almost all the reported methods so far to enhance the

switch's RF performance.

$$S_{21} = \frac{2}{2 + \omega C Z_0} \quad (1)$$

where,  $\omega = (k/m)^{1/2}$  is the resonant frequency;  $C = C_u$  or  $C_d$  is the up-state or down-state capacitance; and  $Z_0$  is the switch's characteristic impedance.

#### 1) SERIES-SHUNT CONFIGURATION

Series-shunt configuration is a common way [26], [29], [55], [56] for RF switches (e.g., p-i-n diodes or FET) to obtain the high-isolation property which and also can be employed by MEMS technology, for both RF-MEMS capacitive and metal-contact switches. For example, two shunt protection contacts connected in front of a series RF-MEMS metal-contact switch, as shown in Fig. 3(a), can increase isolation to around 22dB at frequency of 40GHz although it has a slightly higher insertion loss compared to the unprotected switch due to the additional parasitic capacitance in shunt [37]. Similar approach was also used in [26], [29], [55], [56]; where two shunt metal-contact cantilevers were added on the both sides of the signal line for a series RF-MEMS metal-contact switch, as shown in Fig. 3(b-c). Both cantilevers are pulled down when the switch is open, to short the signal line to the ground line and reduce the parasitic series capacitance

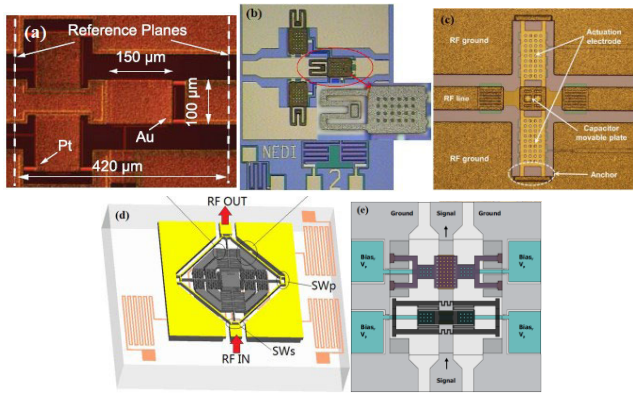


FIGURE 3. RF-MEMS switches with series-shunt configurations: (a) [37], (b) [26], (c) [56], (d) [29] and (e) [59].

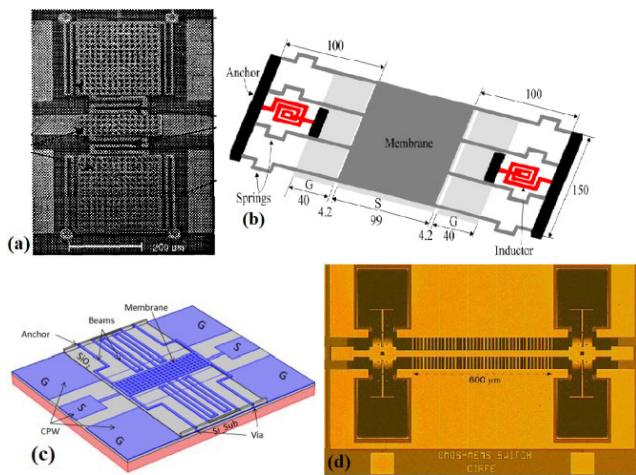


FIGURE 4. RF-MEMS switches with inductive compensation: (a) [60], (b) [47], (c) [14] and (d) [61].

of the metal-contact switch, further to improve its isolation which can be enhanced by at least 10dB in frequency range of DC to 20GHz. A laterally-actuated RF-MEMS metal-contact switch was proposed to use the deformation of a rhombic beam to control the switch which operates in three distinct states (namely on, off and deep-off state), as displayed in Fig. 3(d). The switch’s isolation mechanism of the deep-off state was the series-shunt method and it can reach  $-53\text{dB}$  at 6GHz [29]. Another series-shunt configuration was constructed by a series RF-MEMS metal-contact switch and a shunt RF-MEMS capacitive switch (Fig. 3(e)), each with opposite mechanisms. Simulated results show an excellent isolation of  $-75\text{dB}$  and low insertion loss of  $-0.13\text{dB}$  at 28GHz [59].

2) INDUCTIVE COMPENSATION

For the capacitive RF-MEMS switch, the inductance of the supporting beams and movable membrane play a crucial role in the isolation of the switch since they form inductors connected in series with the RF capacitance [47], [57], [60]. In [60], six single switches each with a different connecting beam but with same area of membrane have been fabricated

and measured. The work claimed that the switch’s high isolation can be obtained with a proper series inductance value of the beam, as shown in Fig. 4(a). Similarly in [47], two inductors were integrated between the movable electrode and ground plane (Fig. 4(b)) to increase its isolation. The most popular inductive compensation methods were reported to be the T-match and Pi-match techniques. The T-match technique is realized by adding two short high-impedance transmission-line sections on either side of the RF-MEMS capacitive switch to improve its isolation. For instance, a T-match RF-MEMS capacitive switch was proposed in [14] (Fig. 4(c)) which can improve the insertion loss and isolation by 55.35% and 24.05%, respectively, compared to the normal switch which does not include the high-impedance transmission-line sections. The Pi-match technique normally consists of two shunt capacitive switches with a high-impedance transmission line section between them, as shown in Fig. 4(d) [61] where the isolation was improved by 53% but the insertion loss was reduced by 30%.

3) LARGE CAPACITANCE RATIO

Equation (1) has clearly shown that the insertion loss and isolation of the RF-MEMS switch are directly proportional with its up-state and down-state capacitance. More precisely, a small up-state capacitance contributes to a little insertion loss; and a large down-state capacitance leads to a high isolation. Therefore, it can be concluded that a large capacitance ratio presents favorable RF performance for RF-MEMS capacitive switch [58]. The capacitance ratio can be theoretically estimated by (2) [14], which indicates the few ways that can be chosen to increase capacitance ratio of the RF-MEMS switch, such as using insulator with high dielectric constant, enlarging air gap, and reducing thickness of the dielectric layer.

$$C_{ratio} = \frac{C_d}{C_u} \approx \frac{g_0 \epsilon_r + t_d}{(1+x)t_d} \tag{2}$$

where,  $g_0$  is the air gap between two electrodes;  $\epsilon_r$  and  $t_d$  is the permittivity and thickness of the dielectric layer, respectively;  $C_d$  and  $C_u$  is down-state and up-state capacitance, respectively; and  $x$  is a coefficient of fringing field capacitance ( $=0.3\sim 0.4$ ).

Use of the insulator materials with high dielectric constant can easily lead to large capacitance ratio design [57], [62], [63]. For example, aluminum nitride (AlN,  $\epsilon_r=9.8$ ) [57], hafnium dioxide ( $\text{HfO}_2$ ,  $\epsilon_r=20\sim 25$ ) [59], [64], tantalum pentoxide ( $\text{Ta}_2\text{O}_5$ ,  $\epsilon_r=32$ ; ( $\text{Ba,Sr})\text{TiO}_3$ ,  $\epsilon_r>200$ ) [57], [65], strontium titanate oxide (STO,  $\epsilon_r=30\sim 120$ ) [66], piezoelectric lead zirconate titanate (PZT,  $\epsilon_r=190$ ) [57] have been used in RF-MEMS capacitive switches before; however, some of them are not easily fabricated and costly. The dielectric thickness should be as small as possible to get a high capacitance ratio. However it could not be less than  $1000\text{\AA}$  due to the pinhole problem and must be able to withstand the pull-in voltage without dielectric breakdown [15]; the typical value is around  $1000\sim 2000\text{\AA}$ . A large air gap also can

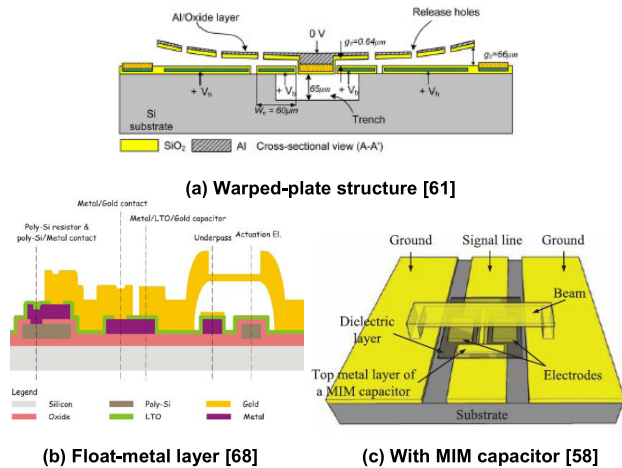


FIGURE 5. Structure designs to increase capacitance ratio.

contribute to a high capacitance ratio; however, big air gap directly leads to a high actuation voltage. Therefore, a trade-off between the capacitance ratio and actuation voltage needs to be considered in an RF-MEMS switch design. In most designs, the air gap switch around  $3\mu\text{m}$  [67].

In addition to the above methods, there are some other ways to increase the RF-MEMS capacitance ratio by modifying its structure. For instance, i) using mechanical stress property of the suspended structure, like beam or membrane with large bending, can increase the capacitance ratio; however, it will lead to a large actuation voltage. In [61], a warped-plate structure (Fig. 5 (a)) is used to increase the switch's capacitance ratio ( $C_d/C_u=91:1$ ) and further to reduce the insertion loss to 0.98dB and increase the isolation to 17.9dB at frequency of 10 to 20GHz. ii) Adding a float metal layer (Fig. 5 (b)) onto the thin dielectric layer underlying the movable electrode is an approach to increase the capacitance ratio by minimizing the effect of surface roughness and curling of movable electrode [68]; Such a metal layer is floating when the switch is not actuated and having no influence on the off-state capacitance value; differently, it serves as capacitor electrode, realizing an ohmic contact with the movable metal when the switch is actuated [56]. iii) Connecting a metal-insulator-metal (MIM) capacitor to the shunt metal-contact switch, as shown in Fig. 5 (c) [58]. When the switch is in the up-state, it consists of two separated capacitors, namely MIM capacitor and metal-air-metal (MAM) capacitor, which are connected in series to realize small insertion loss; when the switch is in the down-state, the MAM capacitor works as a resistor to increase the capacitance and further to increase the capacitance ratio.

#### 4) HIGH RESISTIVITY SUBSTRATE

High resistivity substrate is a necessary requirement for the RF-MEMS switch to obtain good RF performance. For example, high-resistivity silicon [69]–[71], silicon-on-glass (SiOG) [23], gallium arsenide (GaAs) [72], quartz [51], [73], and glass [50] are the common materials used in the

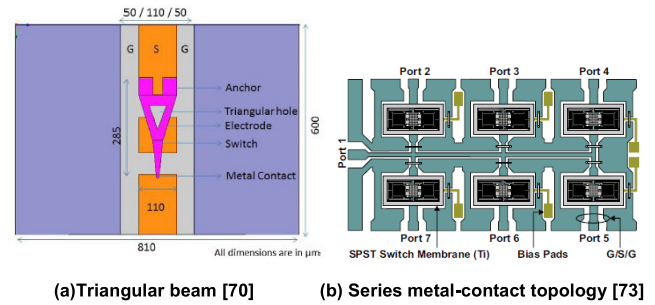


FIGURE 6. High-performance design examples.

RF-MEMS switch's design to reduce the RF loss from the substrate. In order to fabricate the RF-MEMS switches directly on the normal low resistivity silicon substrates which are usually used in the standard CMOS process, a trench under the transmission line and switch design part, as displayed in Fig. 5 (a) is necessary.

#### 5) OTHER APPROACHES

There are also some other design considerations which can be used to improve the RF performance of the RF-MEMS switches. For example, in [70], a suspended triangular gold beam (Fig. 6 (a)) was proposed initially for a series metal-contact RF-MEMS switch with low-actuation voltage. Meanwhile the triangularly shaped beam acts as a tapered transmission line between input and output, which in turn improves the smooth current flow and possibly enhances the return loss and insertion loss characteristics of the switch. In [73], six series RF-MEMS metal-contact switches (Fig. 6 (b)) are designed to get high isolation ( $>45\text{dB}$ ) and low insertion loss ( $-0.01\text{dB}$ ) in frequency of DC to 6GHz, where the membrane and serpentine beams are based on titanium with air gap of only  $1.8\mu\text{m}$ .

#### B. SMALL ACTUATION VOLTAGE

In regards to the driving voltage specification of RF-MEMS switch that can be employed in the upcoming 5G scenario, the RF-MEMS switch's actuation voltage should be controlled within a few volts. These small actuation voltages can also benefit to other properties of the RF-MEMS switch such as reduced interface circuit's complexity and improved switch's reliability [74]. With small actuation voltage, the RF-MEMS switch can be easily and directly implemented into handheld mobile phones, automotive vehicles, and similar wireless devices [75] without external voltage up converter, and further able to decrease the chip size and cost. Moreover, the lifetime of RF-MEMS switch can be improved with low actuation voltage [12], [75] by avoiding the stiction phenomenon and mechanical shock which is caused by high actuation voltage [12], [74]. Although RF-MEMS switch with low actuation voltage has also less mechanical restoring force, the device will tend to be more exposed to stiction and further affecting its reliability; this however can be overcome by proper beam design.



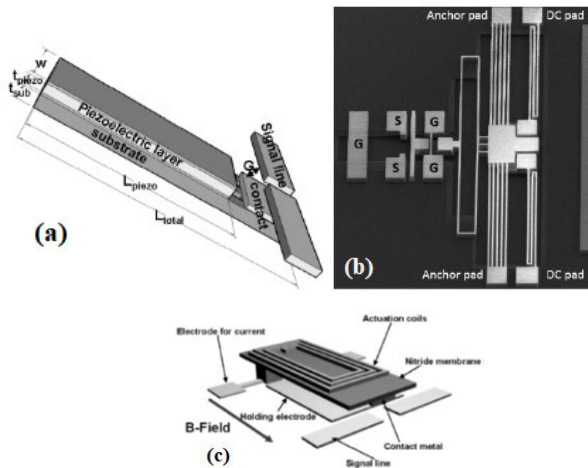


**FIGURE 10.** RF-MEMS switches actuated by different mechanisms: (a) piezoelectric actuated [69], (b) electro-thermal actuated [82], and (c) electromagnetic actuated [85].

switch is around 5V. However, the small air gap affects negatively on the insertion loss [77], due to the non-negligible up-state capacitance [75], especially for the capacitive-type RF-MEMS switch, which can be seen from following design. In [76], the air gap was designed with small value in order to get a low-voltage RF-MEMS switch, but its insertion loss is about  $-2\text{dB}$  from DC to 10GHz. Two methods can be used to overcome this limitation. One approach is to add matching circuits, such as T-match or Pi-match circuits, to compensate the parasitic capacitance, and further to reduce the actuation voltage [62], [77]. The other approach is to design the switch with comb structure and actuated laterally [77].

#### 4) DIFFERENT ACTUATION MECHANISMS

Other than electrostatically-actuated RF-MEMS switches, there are still other actuation mechanisms that can be employed to reduce the actuation voltage. For example, piezoelectric materials can be used to actuate RF-MEMS switch with low pull-in voltage; moreover, the higher piezoelectric coefficient, the lower actuation voltage is desirable [77]. Aluminum nitride (AlN) thin film was used in a metal-contact single-beam RF-MEMS switch with simulated actuation voltage of less than 2V [81]. Lead zirconated titanate (PZT) used for a piezoelectric-actuated RF-MEMS metal-contact switch was presented in [69], where the cantilever actuator was comprised of bottom electrode, PZT layer, and top electrode on silicon nitride cantilever beam (Fig. 10 (a)); and the fabricated switch was successfully operated at 2.5V. Electro-thermal actuation mechanism also can be used to lower the RF-MEMS switch's pull-in voltage. A metal-contact RF-MEMS switch was thermally actuated (Fig. 10 (b)) by pull-in voltage of 11V with big air gap of  $11\mu\text{m}$  [82]. In [83], a lateral RF-MEMS metal-contact latching switch was presented with electro-thermally actuated mechanism which showed the required actuation voltage is only 6V. Electromagnetic RF-MEMS switch generally uses

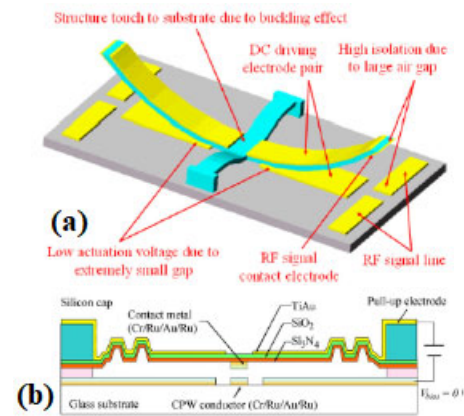


**FIGURE 11.** Other novel low-voltage designs, (a) intrinsically buckled beams [25] and (b) corrugated diaphragm [20].

coil on top of the membrane (Fig. 10 (c)) to generate bend-down force by applying a DC current to the coil. So by modifying the specifications of the coil and membrane, the design with low actuation voltage can be easily achieved, such as actuation voltage of less than 3V in [84], below 5V in [85], and less than 4.3V in [86]. However, this method will increase the switch's power consumption [69].

From these examples, it can be seen that piezoelectric, electro-thermal, and electromagnetic actuated mechanisms for RF-MEMS switches all are possible to present good performance with low-actuation voltages [21]. However, for the piezoelectric RF-MEMS switches, parasitic actuation occurs frequently due to the mismatch in the coefficients of thermal expansion; for the electro-thermal and electromagnetic RF-MEMS switches, their switching time is a bit longer and need more power consumption; moreover, most of them are not compatible with CMOS process.

#### 5) OTHER APPROACHES

Except the aforementioned techniques which can be used for lowering the actuation voltages of the RF-MEMS switches, some other novel methods also have been tried in the reports. In [25], the residual stress was used to intrinsically buckled down the central part of fixed-fixed beam and bending up the free end of the cantilever beams for a suspended crisscross-shape electrode (Fig. 11 (a)) to achieve a low-voltage design meanwhile maintaining a high isolation; compared to the traditional design, its pull-in voltage can be reduced by around 65%. A suspended diaphragm with corrugated feature (Fig. 11 (b)) was used to reduce the pull-in voltage in [20]; comparing with the conventional flat diaphragm design, the pull-in voltage was trimmed down by at least 50%. Graphene-based R-NEMS (radio frequency – nano electro mechanical system) switch is a new direction to obtain the low actuation voltage which can be as low as less than 2V [87]. From the fabrication of point, since the actuation voltage of clamp-clamp beam generally is increased with high residual stress induced during fabrication process especially, lowering the

temperature of the sacrificial layer removal step can significantly reduce the beam's residual stress, at the cost of more time consuming etching step [6]. From the optimization of point, the low-actuation voltage for the RF-MEMS switch can be obtained by optimizing its geometric parameters, such as air gap, beam dimensions, and actuation areas [24], [67].

Many RF-MEMS switches with low-actuation voltage were achieved by combining two or three above mentioned techniques together, for example, i) designs with low spring constant and large actuation area [67], [75]; ii) designs with low spring constant, large actuation area and small air gap [80], [88]; iii) designs with other actuation mechanisms with low spring constant [84]; and so on. All of these methods can come out with a low-voltage RF-MEMS switch's design.

### C. HIGH RELIABILITY

Reliability issue, as one of the major concerns, has prevented many RF-MEMS switches to be commercialized widely and successfully. For metal-contact type, the RF-MEMS switches' reliability is basically limited by micro welding and stiction problem [49], [89]. The switches' typical failure mechanisms include fusing of contacts, metal transfer between contacting surface, increased contact resistance between the moveable contacts and the transmission line, as well as a micro welding problem after repeated actuations [49], [90]. For capacitive type, the RF-MEMS switches' reliability is generally restricted by the stiction between the dielectric layer and the metal, dielectric layer breakdown or mechanical shock due to high actuation voltage, as well as charge injection and charge trapping in the dielectric layers which cause the switch to either stick in the down-state position or increase the actuation voltage [12], [49]. Many different techniques have been adopted to enhance the RF-MEMS metal-contact and capacitive switches, such as employing push-pull mechanics, reducing the pull-in voltage, modifying driving voltage, using hard metal contact, adding shunt protection, proposing non-contact design, minimizing temperature effect, and so on, which have been summarized in detail as follows.

#### 1) EMPLOY PUSH-PULL MECHANISM

The push-pull mechanisms not only can be used together with a small-spring-constant structure for lowering the actuation voltage as mentioned before, but can also be beneficial for improving the switch's reliability through minimizing the stiction phenomenon [53]. Basically, there are four different kinds of push-pull topologies reported so far to avoid electrodes' stiction. One is a large membrane moving in vertical direction and sandwiched by two fixed electrodes (Fig. 8(a)), namely bottom electrode and top electrode, such as the work displayed in [38], [75]. The second way is placing two electrodes on either side of the switch together with a beam suspended by a torsion spring in the middle (Fig. 12); by supplying the voltage to one of them, the switch can be operated like a teeterboard to turn it on or off, as shown the design in [74]. The third topology is designed with two

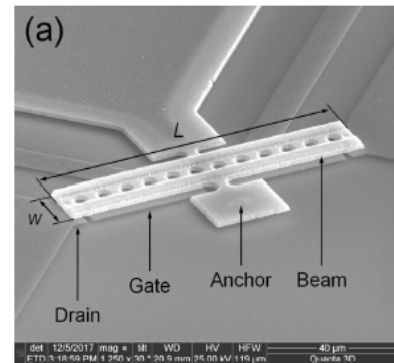


FIGURE 12. RF-MEMS switch based on one torsion spring [74].

pillars supporting a large membrane on it, two electrodes placing inside the pillars and separated by the signal line, and another two electrodes placing outside the pillars, as presented in Fig. 8 (b) [71]. The fourth method is implemented by comb-electrodes moving in lateral direction, as described in Fig. 3 (d) [29].

#### 2) REDUCE PULL-IN VOLTAGE

For capacitive RF-MEMS switch, high operation voltages can cause the charging of the constituent dielectric, which degrades the reliability of the switches [8], [69], [91]. Goldsmith *et al.* reported the lifetime characterization of RF-MEMS capacitive switch in [92], where an exponential relationship between lifetime and actuation voltage exists, namely lifetime between  $10^4$  (65V) and  $10^8$  (30V) switching cycles. According to the results, reducing the pull-in voltage is an effective way to enhance the switch's reliability. For RF-MEMS capacitive switch, lifetime can improve on the order of a decade for every 5 to 7V decrease in applied voltage [33].

#### 3) MODIFY DRIVING VOLTAGE

Developing an actuation strategy for the RF-MEMS switch's operation can lead to enhanced performance with long-term reliability [89]. Bipolar driving voltage is a common way to operate the switch since it can reduce the dielectric charging of the thin insulator layer and further to increase the switch's reliability. In terms of waveforms, the dual-pulse voltage waveform, as compared to sine wave, square wave or triangular wave, is the most effective and popular waveform to actuate the RF-MEMS switches [33], [92], [93], as shown in Fig. 13 (a). The initial pulse, which must be higher than the actuation voltage, provides enough electromotive force to pull the switch membrane down into the on-state. A much lower holding voltage maintains the switch in the down-state to minimize the time of when high voltage is applied across the switch dielectric and further reduce the dielectric charging.

Other than the bipolar dual-pulse driving voltage, another open-loop "soft-landing" waveform (Fig. 13 (b)) can also be used to actuate the RF-MEMS switch with longer lifetime.

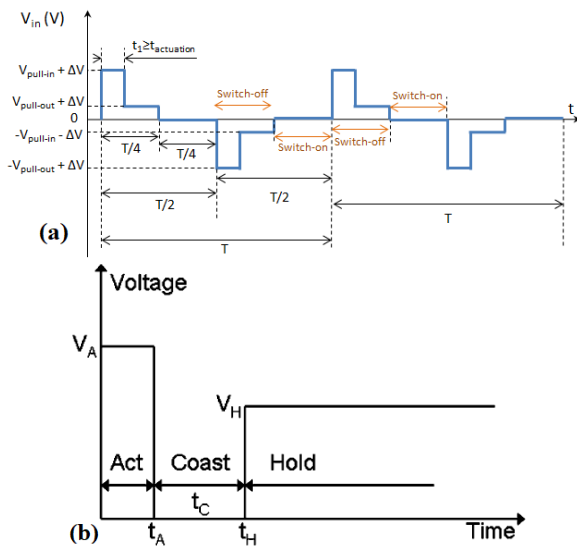


**FIGURE 13.** Suggested driving voltages for RF-MEMS switch's high reliability, (a) two-step bipolar waveform [33], [92], [93] and (b) "soft-landing" waveform [90].

The "soft-landing" waveform consists of an actuation voltage pulse, a coast time, and a hold voltage to achieve nearly zero velocity to close the membrane, avoid the membrane's rebound effect, reduce the impact force imparted on the contacting surfaces upon closure and further to enhance the switch's reliability [90].

#### 4) USE HARD METAL CONTACT

For RF-MEMS metal-contact switch, the reliability can be improved by employing the harder metal contact, such as copper/tungsten/gold stack (Cu/W/Au), rhodium (Re), tungsten (W), molybdenum (Mo), palladium (Pd), silver/tungsten/rhodium (Ag/W/Re), palladium multilayer structures (Ag/Pd, Au/Ag/Pd, Au/Pd), and Ag/W/CdO [20], [94]. Ruthenium/gold (Ru/Au) multilayer has been used for RF-MEMS metal-contact switch, in order to maintain a low contact resistance and enhance its reliability by at least 100 times, compared to the same design using pure-gold contact [20], [28].

#### 5) ADD SHUNT PROTECTION

For a series RF-MEMS metal-contact switch, its reliability can be enhanced by using shunt protection technique, namely using two shunt protection contacts in front of its main contact (Fig. 3 (a)) to block the RF signal and create a local cold-switching condition for the main contact, and then to increase the switch's lifetime under hot-switching condition as presented in [37]. Comparing with the design without shunt protection technique, the enhanced model can improve the lifetime by at least 10 times.

#### 6) PROPOSE NON-CONTACT DESIGN

A novel non-contact RF-MEMS switch based on variable shunt-comb capacitance between the single line and ground

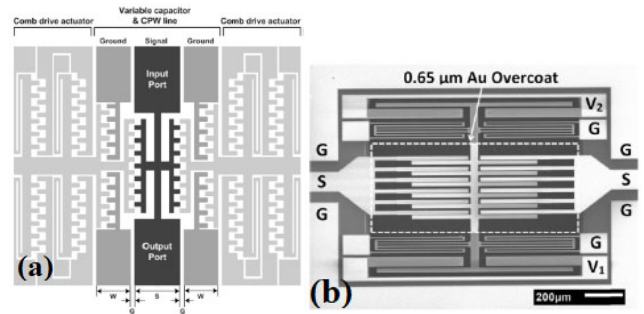


**FIGURE 14.** Non-contact RF-MEMS switches: (a) [49] and (b) [95].

line was presented in Fig. 14 (a) [49] which significantly improves the RF-MEMS switch's reliability by avoiding the charge injection, micro-welding and stiction issues occurring inherently in contact-type RF-MEMS switches. The lifetime can reach  $10^9$  cycles with 18mW RF power input. Similar work has been reported in [95], where the switch is based on variable capacitance between signal lines and movable grounded electrodes controlled by electrostatic actuator, as shown in Fig. 14 (b).

#### 7) MINIMIZE TEMPERATURE EFFECT

The last decade has seen an increase in the development of reliable RF-MEMS switch in terms of reducing their sensitivity to thermal and residual stress [96]. The temperature effect is more sensitive to the clamped-clamped thin film and multilayer structures due to the reaction force. Therefore, several different methods have been used to minimize temperature effect. One way is using thermal compensation structure [28], [96] where a narrow rectangular hole next to each anchor was defined for a thin movable square film to reduce the switch's temperature sensitivity ( $<50\text{mV}/^\circ\text{C}$ ) and ensure it can be operated in a wide temperature range ( $25^\circ\text{C}$  to  $125^\circ\text{C}$ ). The second way is to propose a non-sensitive structure for thermal effect, such as cantilever-based structure [97], thick movable layer and buckle-beam design [28], [97], [98], curved multilayer structures [99]. The third way is employing special materials for the membrane, such as molybdenum [100].

#### 8) OTHER APPROACHES

Apart from the above mentioned techniques which can be used to prolong the lifetime of the RF-MEMS switches, there are still other interesting approaches introduced in related works, such as adding reinforcing-bars-based thick frame on the movable clamp-clamp beam and stopping pillars [101], designing the movable membrane with tri-layer (insulator-metal-insulator) structure [53], placing separated thin posts above the dielectric layer or bottom electrode to eliminate the problem of sticking and to improve the reliability by three orders of magnitude [28], [33], choosing proper dielectric layer (e.g., AlN and PZT which can easily de-trap charges [57]; double-dielectric-layer structures; and small surface roughness) and reducing the temperature changes and humidity effect on it [8], or packaging the switch

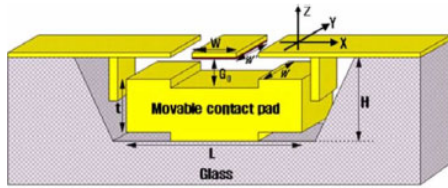


**FIGURE 15.** RF-MEMS switch with freely moving structure [48].

with hermetic methods to avoid the contamination, humidity and destructions [34], [76].

Another novel design for long-lifetime RF-MEMS switch was presented in Fig. 15 [48], where a freely moving contact pad structure was used to actuate the switch through electrostatic force and release it by gravitational force; the switch's lifetime can reach more than 200 billion cycles under cold switching condition; meantime the switch shows a very short switching time ( $1.2\sim 1.3\mu\text{s}$ ) since without any elastic deformation involved in the actuation. The only limitation of this switch is the sensitivity to the slants due to the gravitation.

#### D. SHORT SWITCHING TIME

The RF-MEMS switch's switching time can be reduced by modifying the movable structure, applying proper control voltage, or using different actuation mechanism. For example, normally damping holes (Fig. 9) are formed on the actuation membrane so as to reduce air damping during switch actuation, resulting in an improvement of the switching speed [23]. In [90], a "soft-landing" waveform (Fig. 13 (b)) which can close the membrane with nearly zero velocity and no rebound, as the control voltage for the RF-MEMS switch, could be used to reduce the switch's switching time more than  $30\mu\text{s}$ . Comparing with the electrostatic RF-MEMS switch, piezoelectric actuation shows faster switching speed and low-actuation voltage, but parasitic actuation occurs frequently due to the mismatch in the coefficients of thermal expansion [21].

#### E. MULTIBAND TOPOLOGY

From the frequency specification of the 5G scenario, the RF-MEMS switch with wideband frequency is also a critical factor in some related applications. Several designs have shown the RF-MEMS switches can be developed and operated in wideband frequency. For example, four shunt RF-MEMS capacitive switches with different resonant frequencies were designed to be connected in parallel with small inductive sections (Fig. 16 (a)) to operate in frequency of 11 to 40GHz where its measured isolation is greater than 45dB [60]. A new type of shunt RF-MEMS capacitive switch consists of two cantilever beams which are anchored at the central top electrode of a capacitor (the bottom electrode is the signal line) and hanging over the ground plane (Fig. 16 (b)); this switch can be operated from 3.2 to 20.3GHz by pulling down one beam or two beams together [102]. One more similar idea shunt RF-MEMS capacitive switch was proposed in [103], where a broadside bridge structure

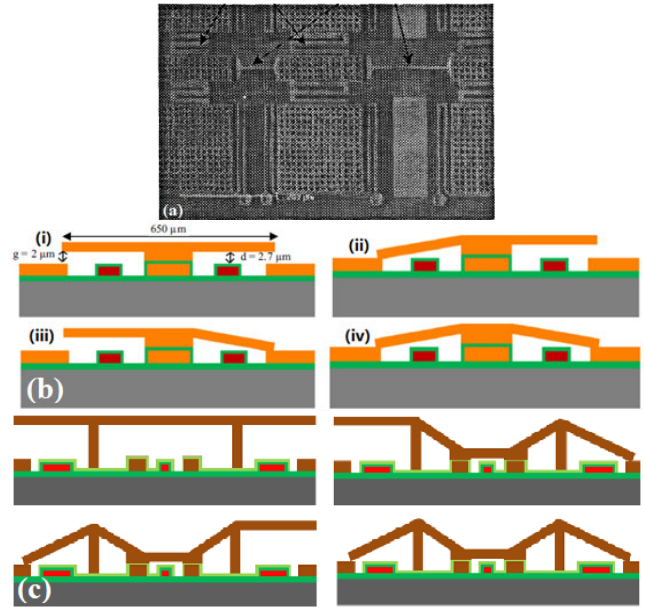


**FIGURE 16.** RF-MEMS switches with multiband characteristic: (a) [60], (b) [102] and (c) [103].

joined with two asymmetric structures of cantilevers on either side (Fig. 16 (c)) was used to operate the switch with four states (namely on state, left-off-state, right-off-state and both-off-state) three resonant peak frequencies of 10.4, 11 and 21.4GHz.

#### F. INTEGRATION AND PACKAGING

The monolithically integrated (e.g., CMOS or BiCMOS based) RF-MEMS switch is a trend for further RF-MEMS switch's development which has shown several advantages, such as i) easily integrated with integration circuits on a single chip, ii) reduced parasitic capacitance, ii) low insertion loss even in very high frequency range (e.g., up to 140GHz, or 250GHz); iii) high isolation; and iv) low fabrication cost since most of them need mask or maskless post-CMOS process [45], [47], [61]. For example, the standard 2P4M (double polysilicon four metal)  $0.35\text{-}\mu\text{m}$  CMOS process from TSMC, and post-process has been used to fabricate RF-MEMS capacitive switch in [45]–[47], [61]; a novel RF CMOS-MEMS switch was fabricated on a  $0.6\text{-}\mu\text{m}$  CMOS LSI (large scale integration) with CMOS control circuits [76]; in [32],  $0.13\mu\text{m}$  SiGe BiCMOS technology was used to fabricate a SPDT switch in 110 to 170GHz. The only limitation of these switches is their high loss from general low resistivity silicon substrate. A trench under the CPW line is suggested to avoid this problem [61]. In order to reduce the contamination and humidity effect to the RF-MEMS switch, a hermetic packaging is preferred. For example, a thin film was used to encapsulate the switch at wafer level in [76] to prevent destruction during other processes and also to enhance the reliability to more than 1 billion cycles; a hermetic chamber made by 20-mm acryl with a range of 0.01 to 1 mbar was employed [34] which shows that the damping coefficient of the switch keeps constant under the pressure condition.

Other than this, using Pyrex or borofloat glass as substrate to fabricate the RF-MEMS switches and then bonding with silicon substrate is another packaging and integrating method, as shown in [50]. Also in [35], a feasible low-cost molded package, namely combining of a silicon-on-insulator (SOI) wafer and an anodic-bonding glass wafer was proposed for the RF-MEMS switch's fabrication; the purpose of the capping is to put the contacts and the actuator under atmospheric control by sealing with nitrogen at reduced pressure to avoid the contamination and humidity effect meantime to increase the lifetime. The main advantage of this method is the ease in the integration of mechanical and electrical components; moreover, the preponderances of the Pyrex glass, such as very high resistivity, small thermal coefficient expansion, and inert to the most of acids and other chemicals, still can be utilized by the RF-MEMS switches' fabrication.

Furthermore, recently based on the development of printable electronics, RF-MEMS capacitive switch can be fabricated using flexible printed circuit processing technique [104] which is suitable for assembly and packaging of RF-MEMS reconfigurable circuits and antennas on laminated substrates, and could show a possible to be transferred and integrated with standard IC systems with low-cost and high-volume approach.

## V. CONCLUSION

Compared to 4G-LTE (4<sup>th</sup> generation – long term evolution) technology, 5G systems demands for wider and higher operation frequency range, as well as larger reconfigurability to cover different services, and can reduce hardware redundancy and power consumption. Scoring such targets means leveraging on passives with boost features, and RF-MEMS technology could be a viable solution, both for 5G RF Front Ends (RFFE) and base stations [13]. RF-MEMS switches, as one of the essential components in wireless communication systems and radar systems, have been thoroughly reviewed in this paper, in terms of their RF performance, actuation voltage, reliability, switching time, multiband topology, integration and packaging. From the design aspect, RF-MEMS capacitive switches generally adopt the shunt-type connection whereas RF-MEMS metal-contact switches uses series-type connection with the transmission line. In order to implement the RF-MEMS switches into 5G related applications, many different techniques in structures, materials, fabrication methods, integrations and packaging have been investigated, summarized and explained in this work. The main contribution of this work is to present an extensive summary which can be referred to for future work in optimizing the RF-MEMS switches' design and performance, especially for 5G and high performance applications.

## REFERENCES

- [1] J. Iannacci, "Internet of Things (IoT); Internet of everything (IoE); tactile Internet; 5G—A (not so evanescent) unifying vision empowered by EH-MEMS (energy harvesting MEMS) and RF-MEMS (radio frequency MEMS)," *Sens. Actuators A, Phys.*, vol. 272, pp. 187–198, Apr. 2018.
- [2] J. Rodriguez, *Fundamentals of 5G Mobile Networks*. Hoboken, NJ, USA: Wiley, 2015.
- [3] Skyworks, "General purpose RF switches," in *Select RF Switches Available From Stock for Prototype or High-Volume Production*. Woburn, MA, USA: Skyworks Solutions, 2017.
- [4] T. Galla. Basics of RF Switches. Analog IC Tips. Accessed: Feb. 25, 2019. [Online]. Available: <https://www.analogictips.com/basics-of-rf-switches/>
- [5] Keysight Technologies, "RF/microwave switching solutions," in *The Core of Test Systems—RF/Microwave Signal Routing Without Compromise*. Santa Rosa, CA, USA: Keysight Technologies, 2017.
- [6] J. Iannacci, "RF-MEMS technology as an enabler of 5G: Low-loss ohmic switch tested up to 110 GHz," *Sens. Actuators A, Phys.*, vol. 279, pp. 624–629, Aug. 2018.
- [7] G. M. Rebeiz and J. B. Muldavin, "RF MEMS switches and switch circuits," *IEEE Microw. Mag.*, vol. 2, no. 4, pp. 59–71, Dec. 2001.
- [8] W. M. Van Spengen, "Capacitive RF MEMS switch dielectric charging and reliability: A critical review with recommendations," *J. Micromech. Microeng.*, vol. 22, no. 7, p. 074001, 2012.
- [9] OMRON Electronic Components. Accessed: Feb. 11, 2019. [Online]. Available: <https://www.components.omron.com/>
- [10] RadantMEMS. Accessed: Dec. 3, 2018. [Online]. Available: <http://www.radantmems.com/>
- [11] L. Wood. *Global Radio Frequency (RF) MEMS Market 2019–2023: Expected to Grow at a CAGR of Approx 37%, With AAC Technologies, Analog Devices, Broadcom, Cavendish Kinetics, and Qorvo at the Forefront-ResearchAndMarkets.com*. Accessed: Feb. 25, 2019. [Online]. Available: <https://www.businesswire.com/news/home/20190221005400/en/Global-Radio-Frequency-RF-MEMS-Market-2019-2023>
- [12] S. Shekhar, K. Vinoy, and G. Ananthasuresh, "Low-voltage high-reliability MEMS switch for millimeter wave 5G applications," *J. Micromech. Microeng.*, vol. 28, no. 7, p. 075012, 2018.
- [13] J. Iannacci, M. Huhn, C. Tschoban, and H. Pötter, "RF-MEMS technology for future mobile and high-frequency applications: Reconfigurable 8-bit power attenuator tested up to 110 GHz," *IEEE Electron Device Lett.*, vol. 37, no. 12, pp. 1646–1649, Dec. 2016.
- [14] L.-Y. Ma, A. N. Nordin, and N. Soin, "A novel design of a low-voltage low-loss T-match RF-MEMS capacitive switch," *Microsyst. Technol.*, vol. 24, no. 1, pp. 561–574, 2018.
- [15] G. M. Rebeiz, *RF MEMS: Theory, Design, and Technology*. Hoboken, NJ, USA: Wiley, 2004.
- [16] J. Iannacci, "RF-MEMS technology: An enabling solution in the transition from 4G-LTE to 5G mobile applications," in *Proc. IEEE Sensors*, Nov. 2017, pp. 1–3.
- [17] GSM Association, "5G spectrum—public policy position," GSMA, London, U.K., White Paper, Nov. 2016.
- [18] A. Osseiran, F. Boccardi, V. Braun, K. Kusume, P. Marsch, M. Maternia, O. Queseth, M. Schellmann, H. Schotten, H. Taoka, H. Tullberg, M. A. Uusitalo, B. Timus, and M. Fallgren, "Scenarios for 5G mobile and wireless communications: The vision of the METIS project," *IEEE Commun. Mag.*, vol. 52, no. 5, pp. 26–35, May 2014.
- [19] J. Iannacci, "RF-MEMS for high-performance and widely reconfigurable passive components—A review with focus on future telecommunications, Internet of Things (IoT) and 5G applications," *J. King Saud Univ.-Sci.*, vol. 29, no. 4, pp. 436–443, 2017.
- [20] F. Ke, J. Miao, and J. Oberhammer, "A ruthenium-based multimetal-contact RF MEMS switch with a corrugated diaphragm," *J. Microelectromech. Syst.*, vol. 17, no. 6, pp. 1447–1459, Dec. 2008.
- [21] W. Tian, P. Li, and L. Yuan, "Research and analysis of MEMS switches in different frequency bands," *Micromachines*, vol. 9, no. 4, p. 185, 2018.
- [22] L. Y. Ma, "Design and analysis of novel low-voltage low loss RF-MEMS switch," Ph.D. dissertation, Dept. Elect. Eng., Univ. Malaya, Kuala Lumpur, Malaysia, 2018.
- [23] J.-M. Kim, J.-H. Park, C.-W. Baek, and Y.-K. Kim, "The SiOG-based single-crystalline silicon (SCS) RF MEMS switch with uniform characteristics," *J. Microelectromech. Syst.*, vol. 13, no. 6, pp. 1036–1042, Dec. 2004.
- [24] J.-M. Kim, S. Lee, J.-H. Park, C.-W. Baek, Y. Kwon, and Y.-K. Kim, "Electrostatically driven low-voltage micromechanical RF switches using robust single-crystal silicon actuators," *J. Micromech. Microeng.*, vol. 20, no. 9, p. 095007, 2010.
- [25] C.-H. Chu, W.-P. Shih, S.-Y. Chung, H.-C. Tsai, T.-K. Shing, and P.-Z. Chang, "A low actuation voltage electrostatic actuator for RF MEMS switch applications," *J. Micromech. Microeng.*, vol. 17, p. 1649, Jul. 2007.

- [26] Y.-W. Yu, J. Zhu, S.-X. Jia, and Y. Shi, "A high isolation series-shunt RF MEMS switch," *Sensors*, vol. 9, no. 6, pp. 4455–4464, 2009.
- [27] C. D. Patel and G. M. Rebeiz, "An RF-MEMS switch for high-power applications," in *IEEE/MTT-S Int. Microw. Symp. Dig.*, Jun. 2012, pp. 1–3.
- [28] C. D. Patel and G. M. Rebeiz, "A high-reliability high-linearity high-power RF MEMS metal-contact switch for DC–40-GHz applications," *IEEE Trans. Microw. Theory Techn.*, vol. 60, no. 10, pp. 3096–3112, Oct. 2012.
- [29] L. F. Wang, L. Han, J. Y. Tang, and Q. A. Huang, "Lateral contact three-state RF MEMS switch for ground wireless communication by actuating rhombic structures," *J. Microelectromech. Syst.*, vol. 22, no. 1, pp. 10–12, Feb. 2013.
- [30] S. S. Attar, S. Setoodeh, R. R. Mansour, and D. Gupta, "Low-temperature superconducting DC-contact RF MEMS switch for cryogenic reconfigurable RF front-ends," *IEEE Trans. Microw. Theory Techn.*, vol. 62, no. 7, pp. 1437–1447, Jun. 2014.
- [31] J. Sun, Z. Li, J. Zhu, Y. Yu, and L. Jiang, "Design of DC-contact RF MEMS switch with temperature stability," *AIP Adv.*, vol. 5, no. 4, p. 041313, 2015.
- [32] S. T. Wipf, A. Göritz, M. Wietstruck, C. Wipf, B. Tillack, and M. Kaynak, "D-band RF-MEMS SPDT switch in a 0.13  $\mu\text{m}$  SiGe BiCMOS technology," *IEEE Microw. Wireless Compon. Lett.*, vol. 26, no. 12, pp. 1002–1004, Dec. 2016.
- [33] R. Chan, R. Lesnick, D. Becher, and M. Feng, "Low-actuation voltage RF MEMS shunt switch with cold switching lifetime of seven billion cycles," *J. Microelectromech. Syst.*, vol. 12, no. 5, pp. 713–719, Oct. 2003.
- [34] J. Lee, C. H. Je, S. Kang, and C. Choi, "A low-loss single-pole six-throw switch based on compact RF MEMS switches," *IEEE Trans. Microw. Theory Techn.*, vol. 53, no. 11, pp. 3335–3344, Nov. 2005.
- [35] T. Seki, Y. Uno, K. Narise, T. Masuda, K. Inoue, S. Sato, F. Sato, K. Imanaka, and S. Sugiyama, "Development of a large-force low-loss metal-contact RF MEMS switch," *Sens. Actuators A, Phys.*, vol. 132, no. 2, pp. 683–688, 2006.
- [36] D. Yamane, W. Sun, H. Seit, S. Kawasaki, H. Fujita, and H. Toshiyoshi, "A Ku-band dual-SPDT RF-MEMS switch by double-side SOI bulk micromachining," *J. Microelectromech. Syst.*, vol. 20, no. 5, pp. 1211–1221, 2011.
- [37] Y. Liu, Y. Bey, and X. Liu, "High-power high-isolation RF-MEMS switches with enhanced hot-switching reliability using a shunt protection technique," *IEEE Trans. Microw. Theory Techn.*, vol. 65, no. 9, pp. 3188–3199, Sep. 2017.
- [38] D. Peroulis, S. P. Pacheco, and L. P. B. Katehi, "RF MEMS switches with enhanced power-handling capabilities," *IEEE Trans. Microw. Theory Techn.*, vol. 52, no. 1, pp. 59–68, Jan. 2004.
- [39] D. Bansal, A. Bajpai, P. Kumar, M. Kaur, A. Kumar, A. Chandran, and K. Rangra, "Low voltage driven RF MEMS capacitive switch using reinforcement for reduced buckling," *J. Micromech. Microeng.*, vol. 27, no. 2, p. 024001, 2016.
- [40] A. Chakraborty and B. Gupta, "Utility of RF MEMS miniature switched capacitors in phase shifting applications," *AEU-Int. J. Electron. Commun.*, vol. 75, pp. 98–107, May 2017.
- [41] X. Rottenberg, H. Jansen, B. Nauwelaers, P. Fiorini, W. De Raedt, and H. Tilmans, "Boosted RF-MEMS capacitive shunt switches," in *Proc. Workshop Semiconductor Sensor Actuator (SeSens)*, Veldhoven, The Netherlands, 2002, pp. 667–671.
- [42] S. Shekhar, K. J. Vinoy, and G. K. Ananthasuresh, "Design, fabrication and characterization of capacitive RF MEMS switches with low pull-in voltage," in *Proc. IEEE Int. Microw. RF Conf. (IMaRC)*, Dec. 2014, pp. 182–185.
- [43] K. Rangra, B. Margesin, L. Lorenzelli, F. Giacomozzi, C. Collini, M. Zen, G. Soncini, L. del Tin, and R. Gaddi, "Symmetric toggle switch—A new type of rf MEMS switch for telecommunication applications: Design and fabrication," *Sens. Actuators A, Phys.*, vol. 123, pp. 505–514, Sep. 2005.
- [44] H.-H. Yang, H. Zareie, and G. M. Rebeiz, "A high power stress-gradient resilient RF MEMS capacitive switch," *J. Microelectromech. Syst.*, vol. 24, no. 3, pp. 599–607, Jul. 2015.
- [45] C.-L. Dai, H.-J. Peng, M.-C. Liu, C.-C. Wu, and L.-J. Yang, "Design and fabrication of RF MEMS switch by the CMOS process," *Airiti Library*, vol. 8, no. 3, pp. 197–202, 2005.
- [46] C.-L. Dai and J.-H. Chen, "Low voltage actuated RF micromechanical switches fabricated using CMOS-MEMS technique," *Microsyst. Technol.*, vol. 12, no. 12, pp. 1143–1151, 2006.
- [47] C.-L. Dai and Y.-L. Chen, "Modeling and manufacturing of micromechanical RF switch with inductors," *Sensors*, vol. 7, no. 11, pp. 2660–2670, 2007.
- [48] S.-D. Lee, B.-C. Jun, S.-D. Kim, H.-C. Park, J.-K. Rhee, and K. Mizuno, "An RF-MEMS switch with low-actuation voltage and high reliability," *J. Microelectromech. Syst.*, vol. 15, no. 6, pp. 1605–1611, 2006.
- [49] J. Park, E. S. Shim, W. Choi, Y. Kim, Y. Kwon, and D.-I. Cho, "A non-contact-type RF MEMS switch for 24-GHz radar applications," *J. Microelectromech. Syst.*, vol. 18, no. 1, pp. 163–173, Feb. 2009.
- [50] S. Jaibir, K. Nagendra, and D. Amitava, "Fabrication of low pull-in voltage RF MEMS switches on glass substrate in recessed CPW configuration for V-band application," *J. Micromech. Microeng.*, vol. 22, no. 2, p. 025001, 2012.
- [51] K. Demirel, E. Yazgan, Ş. Demir, and T. Akin, "A folded leg Ka-band RF MEMS shunt switch with amorphous silicon (a-Si) sacrificial layer," *Microsyst. Technol.*, vol. 23, no. 5, pp. 1191–1200, 2016.
- [52] M. Li, J. Zhao, Z. You, and G. Zhao, "Design and fabrication of a low insertion loss capacitive RF MEMS switch with novel micro-structures for actuation," *Solid-State Electron.*, vol. 127, pp. 32–37, Jan. 2017.
- [53] V. Kumar, S. K. Koul, and A. Basu, "RF MEMS switch with enhanced reliability," in *Proc. IEEE Int. Symp. Radio-Freq. Integr. Technol. (RFIT)*, Aug. 2018, pp. 1–3.
- [54] R. Kumar and O. Pertin, "Design of an improved micro-electromechanical-systems switch for RF communication system," in *Recent Trends in Communication, Computing, and Electronics*. Singapore: Springer, 2019, pp. 3–13.
- [55] F. Casini, P. Farinelli, G. Mannocchi, S. DiNardo, B. Margesin, G. De Angelis, R. Marcelli, O. Vendier, and L. Vietzorreck, "High performance RF-MEMS SP4T switches in CPW technology for space applications," in *Proc. IEEE Eur. Microw. Conf. (EuMC)*, Sep. 2010, pp. 89–92.
- [56] J. Iannacci, G. Resta, P. Farinelli, and R. Sorrentino, "RF-MEMS components and networks for high-performance reconfigurable telecommunication and wireless systems," *Adv. Sci. Technol.*, vol. 81, pp. 65–74, Sep. 2013.
- [57] M. F.-B. Badia, E. Buitrago, and A. M. Ionescu, "RF MEMS shunt capacitive switches using AlN compared to Si<sub>3</sub>N<sub>4</sub> dielectric," *J. Microelectromech. Syst.*, vol. 21, no. 5, pp. 1229–1240, 2012.
- [58] H. Wei, Z. Deng, X. Guo, Y. Wang, and H. Yang, "High on/off capacitance ratio RF MEMS capacitive switches," *J. Micromech. Microeng.*, vol. 27, no. 5, p. 055002, 2017.
- [59] T. Singh, "Design and finite element modeling of series-shunt configuration based RF MEMS switch for high isolation operation in K–Ka band," *J. Comput. Electron.*, vol. 14, no. 1, pp. 167–179, 2015.
- [60] D. Peroulis, S. Pacheco, K. Sarabandi, and P. Katehi, "MEMS devices for high isolation switching and tunable filtering," in *IEEE MTT-S Int. Microw. Symp. Dig.*, vol. 2, Jun. 2000, pp. 1217–1220.
- [61] S. Fouladi and R. R. Mansour, "Capacitive RF MEMS switches fabricated in standard 0.35  $\mu\text{m}$  CMOS technology," *IEEE Trans. Microw. Theory Techn.*, vol. 58, no. 2, pp. 478–486, Feb. 2010.
- [62] S. Afrang and E. Abbaspour-Sani, "A low voltage MEMS structure for RF capacitive switches," *Prog. Electromagn. Res.*, vol. 65, pp. 157–167, 2006.
- [63] K. Guha, M. Kumar, A. Parmar, and S. Baishya, "Non uniform meander based low actuation voltage high capacitance ratio RF MEMS shunt capacitive switch," in *Proc. IEEE 9th Nanotechnol. Mater. Devices Conf. (NMDC)*, Oct. 2014, pp. 120–123.
- [64] M. Angira, G. Sundaram, K. Rangra, D. Bansal, and M. Kaur, "On the investigation of an interdigitated, high capacitance ratio shunt RF-MEMS switch for X-band applications," in *Proc. NSTI Nanotech*, Washington, DC, USA, vol. 2, 2013, pp. 189–192.
- [65] A. Persano, A. Cola, G. De Angelis, A. Taurino, P. Siciliano, and F. Quaranta, "Capacitive RF MEMS switches with tantalum-based materials," *J. Microelectromech. Syst.*, vol. 20, no. 2, pp. 365–370, 2011.
- [66] J. Y. Park, G. H. Kim, K. W. Chung, and J. U. Bu, "Fully integrated micromachined capacitive switches for RF applications," in *IEEE MTT-S Int. Microw. Symp. Dig.*, vol. 1, Jun. 2000, pp. 283–286.
- [67] L.-Y. Ma, A. N. Nordin, and N. Soin, "Design, optimization and simulation of a low-voltage shunt capacitive RF-MEMS switch," *Microsyst. Technol.*, vol. 22, no. 3, pp. 537–549, Apr. 2016.
- [68] C. Calaza, B. Margesin, F. Giacomozzi, K. Rangra, and V. Mulloni, "Electromechanical characterization of low actuation voltage RF MEMS capacitive switches based on DC CV measurements," *Microelectron. Eng.*, vol. 84, nos. 5–8, pp. 1358–1362, May/Aug. 2007.
- [69] H.-C. Lee, J.-Y. Park, and J.-U. Bu, "Piezoelectrically actuated RF MEMS DC contact switches with low voltage operation," *IEEE Microw. Wireless Compon. Lett.*, vol. 15, no. 4, pp. 202–204, Apr. 2005.

- [70] A. Gopalan and U. K. Kommuri, "Design and development of miniaturized low voltage triangular RF MEMS switch for phased array application," *Appl. Surf. Sci.*, vol. 449, pp. 340–345, Aug. 2018.
- [71] S. Touati, N. Lorphelin, A. Kancierzewski, R. Robin, A.-S. Rollier, O. Millet, and K. Segueni, "Low actuation voltage totally free flexible RF MEMS switch with antistiction system," in *Proc. IEEE Symp. Design, Test, Integr. Packag. MEMS/MOEMS*, Apr. 2008, pp. 66–70.
- [72] A. Persano, A. Tazzoli, P. Farinelli, G. Meneghesso, P. Siciliano, and F. Quaranta, "K-band capacitive MEMS switches on GaAs substrate: Design, fabrication, and reliability," *Microelectron. Rel.*, vol. 52, nos. 9–10, pp. 2245–2249, 2012.
- [73] T. Singh and K. J. Rangra, "Compact low-loss high-performance single-pole six-throw RF MEMS switch design and modeling for DC to 6 GHz," *Microsyst. Technol.*, vol. 21, pp. 2387–2396, Nov. 2015.
- [74] I. V. Uvarov and A. N. Kupriyanov, "Stiction-protected MEMS switch with low actuation voltage," *Microsyst. Technol.*, vol. 25, no. 8, pp. 3243–3251, 2018.
- [75] D. Peroulis, S. P. Pacheco, K. Sarabandi, and L. P. B. Katehi, "Electromechanical considerations in developing low-voltage RF MEMS switches," *IEEE Trans. Microw. Theory Techn.*, vol. 51, no. 1, pp. 259–270, Jan. 2003.
- [76] K. Kuwabara, N. Sato, T. Shimamura, H. Morimura, J. Kodate, T. Sakata, S. Shigematsu, K. Kudou, K. Machida, M. Nakanishi, and H. Ishii, "RF CMOS-MEMS switch with low-voltage operation for single-chip RF LSIs," in *IEDM Tech. Dig.*, Dec. 2006, pp. 1–4.
- [77] Y. Mafinejad, A. Kouzani, K. Mafinezhad, and I. Mashad, "Review of low actuation voltage RF MEMS electrostatic switches based on metallic and carbon alloys," *J. Microelectron., Electron. Compon. Mater.*, vol. 43, no. 2, pp. 85–96, 2013.
- [78] H. Jaafar, O. Sidek, A. Miskam, and S. Korakkottil, "Design and simulation of microelectromechanical system capacitive shunt switches," *Amer. J. Eng. Appl. Sci.*, vol. 2, no. 4, pp. 655–660, 2009.
- [79] R. Kaur, C. Tripathi, and D. Kumar, "Low voltage RF MEMS capacitive shunt switches," *Wireless Pers. Commun.*, vol. 78, no. 2, pp. 1391–1401, 2014.
- [80] F. Guo, Z. Zhiqiang, Y. F. Long, W. M. Wang, S. Zhu, Z. S. Lai, N. Li, G. Q. Yang, and W. Lu, "Study on low voltage actuated MEMS rf capacitive switches," *Sens. Actuators A, Phys.*, vol. 108, nos. 1–3, pp. 128–133, 2003.
- [81] M. H. Ziko and A. Koel, "Design and optimization of AlN based RF MEMS switches," *IOP Conf. Series, Mater. Sci. Eng.*, vol. 362, p. 012002, May 2018.
- [82] D. Shojaei-Asanjan, M. Bakri-Kassem, and R. R. Mansour, "Analysis of thermally actuated RF-MEMS switches for power limiter applications," *J. Microelectromech. Syst.*, vol. 28, no. 1, pp. 107–113, Feb. 2019.
- [83] E. Pirmoradi, H. Mirzajani, and H. B. Ghavifekr, "Design and simulation of a novel electro-thermally actuated lateral RF MEMS latching switch for low power applications," *Microsyst. Technol.*, vol. 21, no. 2, pp. 465–475, 2015.
- [84] Y.-H. Zhang, G. Ding, X. Shun, D. Gu, B. Cai, and Z. Lai, "Preparing of a high speed bistable electromagnetic RF MEMS switch," *Sens. Actuators A, Phys.*, vol. 134, no. 2, pp. 532–537, 2007.
- [85] I.-J. Cho, T. Song, S.-H. Baek, and E. Yoon, "A low-voltage and low-power RF MEMS series and shunt switches actuated by combination of electromagnetic and electrostatic forces," *IEEE Trans. Microw. Theory Techn.*, vol. 53, no. 7, pp. 2450–2457, Jul. 2005.
- [86] I.-J. Cho and E. Yoon, "Design and fabrication of a single membrane push-pull SPDT RF MEMS switch operated by electromagnetic actuation and electrostatic hold," *J. Micromech. Microeng.*, vol. 20, no. 3, p. 035028, 2010.
- [87] P. Sharma, J. Perruisseau-Carrier, C. Moldovan, and A. M. Ionescu, "Electromagnetic Performance of RF NEMS Graphene Capacitive Switches," *IEEE Trans. Nanotechnol.*, vol. 13, no. 1, pp. 70–79, Jan. 2014.
- [88] K. S. Rao, L. N. Thalluri, K. Guha, and K. G. Sravani, "Fabrication and characterization of capacitive RF MEMS perforated switch," *IEEE Access*, vol. 6, pp. 77519–77528, 2018.
- [89] Z. Guo, N. McGruer, and G. Adams, "Modeling, simulation and measurement of the dynamic performance of an ohmic contact, electrostatically actuated RF MEMS switch," *J. Micromech. Microeng.*, vol. 17, no. 9, p. 1899, 2007.
- [90] D. A. Czaplowski, C. W. Dyck, H. Sumali, J. E. Massad, J. D. Kuppers, I. Reines, W. D. Cowan, and C. P. Tigges, "A soft-landing waveform for actuation of a single-pole single-throw ohmic RF MEMS switch," *J. Microelectromech. Syst.*, vol. 15, no. 6, pp. 1586–1594, Dec. 2006.
- [91] V. B. Sawant, M. Madhewar, A. Anjum, and S. S. Mohite, "Modeling and analysis of low voltage, high isolation capacitive type RF-MEMS switches," in *Proc. IEEE 9th Int. Conf. Comput., Commun. Netw. Technol. (ICCCNT)*, Jul. 2018, pp. 1–6.
- [92] C. Goldsmith, J. Ehmke, A. Malczewski, B. Pillans, S. Eshelman, Z. Yao, J. Brank, and M. Eberly, "Lifetime characterization of capacitive RF MEMS switches," in *IEEE MTT-S Int. Microw. Symp. Dig.*, vol. 1, May 2001, pp. 227–230.
- [93] M. L. Ya, N. Soin, and A. N. Nordin, "Theoretical and simulated investigation of dielectric charging effect on a capacitive RF-MEMS switch," in *Proc. IEEE Int. Conf. Semiconductor Electron. (ICSE)*, Aug. 2016, pp. 17–20.
- [94] J. Pal, Y. Zhu, J. Lu, D. Dao, and F. Khan, "High power and reliable SPST/SP3T RF MEMS switches for wireless applications," *IEEE Electron Device Lett.*, vol. 37, no. 9, pp. 1219–1222, Sep. 2016.
- [95] J. Pal, Y. Zhu, J. Lu, F. Khan, and D. Dao, "A novel three-state contactless RF micromachined switch for wireless applications," *IEEE Electron Device Lett.*, vol. 36, no. 12, pp. 1363–1365, Dec. 2015.
- [96] R. Mahameed and G. M. Rebeiz, "RF MEMS capacitive switches for wide temperature range applications using a standard thin-film process," *IEEE Trans. Microw. Theory Techn.*, vol. 59, no. 7, pp. 1746–1752, Jul. 2011.
- [97] A. Grichener and G. M. Rebeiz, "High-reliability RF-MEMS switched capacitors with digital and analog tuning characteristics," *IEEE Trans. Microw. Theory Techn.*, vol. 58, no. 10, pp. 2692–2701, Sep. 2010.
- [98] M. A. El-Tanani and G. M. Rebeiz, "High-performance 1.5–2.5-GHz RF-MEMS tunable filters for wireless applications," *IEEE Trans. Microw. Theory Techn.*, vol. 58, no. 6, pp. 1629–1637, Jun. 2010.
- [99] M. Bakri-Kassem, S. Fouladi, and R. R. Mansour, "Novel High-Q MEMS curled-plate variable capacitors fabricated in 0.35- $\mu\text{m}$  CMOS technology," *IEEE Trans. Microw. Theory Techn.*, vol. 56, no. 2, pp. 530–541, Feb. 2008.
- [100] C. Goldsmith, D. Forehand, D. Scarbrough, I. Johnston, S. Sampath, A. Datta, Z. Peng, C. Palego, and J. C. M. Hwang, "Performance of molybdenum as a mechanical membrane for RF MEMS switches," in *IEEE MTT-S Int. Microw. Symp. Dig.*, Jun. 2009, pp. 1229–1232.
- [101] V. Mulloni, F. Solazzi, G. Resta, F. Giacomozzi, and B. Margesin, "RF-MEMS switch design optimization for long-term reliability," *Analog Integr. Circuits Signal Process.*, vol. 78, no. 2, pp. 323–332, 2014.
- [102] M. Angira and K. Rangra, "A low insertion loss, multi-band, fixed central capacitor based RF-MEMS switch," *Microsyst. Technol.*, vol. 21, no. 10, pp. 2259–2264, 2015.
- [103] M. Angira, G. Sundaram, and K. J. Rangra, "A novel approach for low insertion loss, multi-band, capacitive shunt RF-MEMS switch," *Wireless Pers. Commun.*, vol. 83, no. 3, pp. 2289–2301, 2015.
- [104] R. Ramadoss, S. Lee, Y. C. Lee, V. M. Bright, and K. C. Gupta, "Fabrication, assembly, and testing of RF MEMS capacitive switches using flexible printed circuit technology," *IEEE Trans. Adv. Packag.*, vol. 26, no. 3, pp. 248–254, Aug. 2003.



**LI-YA MA** received the B.Eng. degree in electronic and information engineering from Changchun University, Jilin, China, the M.S. degree in electronics engineering from International Islamic University Malaysia, and the Ph.D. degree in electronic engineering from the University of Malaya, Kuala Lumpur, Malaysia, in 2018, where she is currently a Postdoctoral Research Fellow with the Faculty of Engineering. Her research interests include microelectromechanical systems

(MEMS), RF-MEMS switches, finite-element modeling, microelectronics, and very large-scale integration (VLSI) technology. Her current research has been extended to the fabrication and characterization of flexible electronics, which contain printable fabrication methods and materials and flexible and stretchable sensors with electrodes.



**NORHAYATI SOIN** received the B.Eng. degree (Hons.) in electrical and electronic engineering from Liverpool University, U.K., in 1991, the M.Sc. degree in microelectronic and IT from Liverpool John Moores University, in 1999, and the Ph.D. degree from Universiti Kebangsaan Malaysia, in 2006. She is currently a Professor with the Department of Electrical Engineering, Faculty of Engineering, University of Malaya, where she is also the Director of the Centre of

Printable Electronics. She has published two books and more than 350 articles. Her research interests include microelectronics (reliability of integrated circuit and semiconductor devices, IC design, and semiconductor device modeling), RF microelectromechanical systems (MEMS), BIOMEMS, and flexible and printable electronics. She has been the Chair of the IEEE Electron Devices Society Malaysia Chapter, since 2019.



**SHARIFAH FATMADIANA WAN MUHAMAD HATTA** received the M.Eng. degree majoring in solid-state devices from The University of Sheffield, the M.Sc. degree in microelectronics from the University of Malaya, and the Ph.D. degree in microelectronics from Liverpool John Moores University, U.K. She is currently focusing on emerging technologies in nanoelectronics devices.

...



**MOHAMAD HAZWAN MOHD DAUT** received the M.Eng. degree (Hons.) in electrical engineering from The University of Sheffield, U.K., in 2013, and the Ph.D. degree in engineering from the University of Cambridge, U.K., in 2019. His research interests include the design and development of low-power energy harvesting systems, including energy harvesting mechanisms, low-power converters, and power flow control for paralleling multiple low-power dc–dc converters. His research also covers the fabrication and characterization of thin-film devices based on oxide semiconductors for the applications of flexible power circuits for low-power applications.